

Dynamics of blinking vortices

Anton Daitche

Institute for Theoretical Physics, Münster University, Wilhelm-Klemm-Strasse 9, D-48149, Germany

Tamás Tél

Institute for Theoretical Physics, Eötvös University, P.O. Box 32, H-1518 Budapest, Hungary

(Received 13 May 2008; revised manuscript received 9 September 2008; published 20 January 2009)

We investigate the dynamics of N moving point vortices, whose vorticity changes periodically between a finite value and zero. The dynamics of such blinking vortices is chaotic, but the degree of chaoticity, expressed in terms of finite size Lyapunov exponents, decreases monotonically with time. In contrast to traditional point vortices, the average diameter of the blinking vortex system increases in time. The average size follows a subdiffusive power law scaling $\sim t^\sigma$, with $\sigma < 1/2$. This expanding vortex system provides a flow which is in between closed and open flows. The advection dynamics generated by the blinking vortices is also studied, and leads to dye distribution patterns which are much more realistic than those of the classical point vortex problems, and can be characterized by a dimension less than 2.

DOI: [10.1103/PhysRevE.79.016210](https://doi.org/10.1103/PhysRevE.79.016210)

PACS number(s): 05.45.-a, 47.52.+j, 47.53.+n

I. INTRODUCTION

Systems of two-dimensional point vortices are known to exhibit chaotic motion if they contain four or more vortices (see, e.g., [1]). The advection dynamics of passive particles is already chaotic in the field of three vortices. With the exception of cases where the overall vorticity is zero, the average vortex distance remains constant, and is on the order of the average initial distance among the vortices. Advected particles might depart further away but there is a maximum distance from the vortices, the diameter of the chaotic sea, which is also on the order of the average vortex distance. The question arises how one can generate efficient mixing by vortices in an extended region of a fluid, much larger than the initial vortex distance.

The blinking vortex model [2] and its variants [3,4] have become paradigms of chaotic advection. They consist of two vortices, which are active in an alternating fashion, and the vortex centers are fixed. We remove this constraint so that the vortex centers can *move*, and extend the model to more than two vortices. The centers of the inactive vortices are fluid elements which are advected by the field of the active vortices. The dynamics of such vortices is quite rich even for $N=2$.

We shall mainly be interested in $N > 4$ blinking vortices, out of which at least four are typically active at any instant of time. This ensures that the vortex dynamics is always chaotic. The inactive centers are advected in a chaotic fashion, too, and when they revive, the new vortex appears at a seemingly random site. Thus what we expect to see is a complex motion of the vortex centers around which new vortices show up randomly, while some of the active ones die. The finite lifetime of vortices and the appearance of new ones at unexpected sites is characteristic of realistic flows, like, e.g., two-dimensional turbulence [5,6].

The paper is organized as follows. In the next section the blinking vortex model is defined, and the numerical results concerning the dynamics of the vortex centers are presented in Sec. III. Section IV deals with the temporal change of the finite size Lyapunov exponent. Next, the advection dynamics

is reviewed. In Sec. VI the parameter dependence is investigated and a scaling law is derived. The last Section is devoted to a discussion where a qualitative comparison with decaying turbulence is also given. In the Appendix a possible uniform motion of two blinking vortices is analyzed, which turns out to determine the long term dynamics of the problem of N blinking vortices.

II. THE BLINKING VORTEX MODEL

The flow velocity around a vortex center depends on the distance r from the center as $1/r$. The velocity components around a single vortex centered at the origin are thus

$$v_x = -K \frac{y}{r^2}, \quad v_y = K \frac{x}{r^2}, \quad (1)$$

where $r = \sqrt{x^2 + y^2}$. The parameter K denotes the vortex strength. If there is more than one vortex, none of them remains in place, since each vortex is advected by the flow generated by the others. The motion of the vortex centers can be determined from the solution of a differential equation.

In the presence of N permanent vortices, let (x_i, y_i) and K_i denote the positions of the vortex centers and the vortex strengths, respectively. An elementary derivation of the differential equations governing the dynamics of the vortex centers is given, e.g., in [8] and yields

$$\dot{x}_i = - \sum_{j \neq i}^N K_j \frac{y_i - y_j}{r_{i,j}^2}, \quad \dot{y}_i = \sum_{j \neq i}^N K_j \frac{x_i - x_j}{r_{i,j}^2}, \quad (2)$$

where

$$r_{i,j} = \sqrt{(x_i - x_j)^2 + (y_i - y_j)^2} \quad (3)$$

denotes the distance between vortex i and j . When measuring time and distance in appropriate time and length units, the vortex strengths are also dimensionless. These equations remain valid for time-dependent vortex strengths, too, just K_j should be replaced by $K_j(t)$.

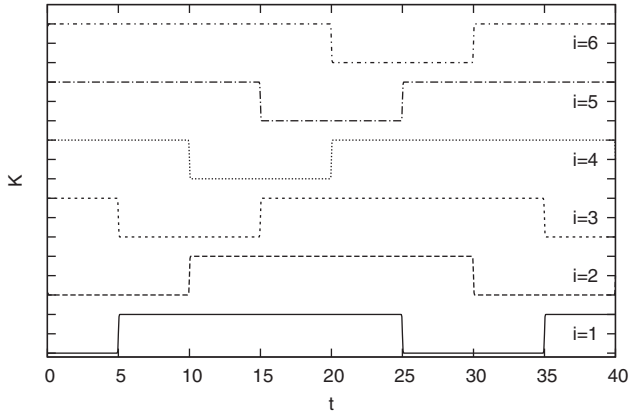


FIG. 1. The different vortex strengths $K_i(t)$, $i=1, \dots, 6$ of the blinking six-vortex model in the time interval $0 < t < 8T$ with $T=5$, $a=69.1$.

The blinking vortex dynamics is obtained by choosing the vortex strength K_j to be time-periodic. The (dimensionless) length of inactive periods will be denoted by $2T$, and T is called the blinking time. For simplicity, we take all the active vortices of equal strength, of value unity. The different vortex strengths can thus be expressed by the same function $K(t)$, taken at different phase shifts. Function $K(t)$ should have a rapid crossover between values 1 and 0.

In the bulk of the paper we deal with $N=6$ blinking vortices out of which at least four are active at any instant of time. The different functions $K_i(t)$ can then be chosen as

$$K_i[t] = K[t - (i-2)T], \quad i = 1, \dots, 6, \quad (4)$$

where $K[t]$ is a function of period $6T$ (the active periods are of length $4T$). We have used the particular form ($0 < t < 6T$)

$$K(t) = \frac{1}{e^{at} - 1} + \frac{1}{e^{-a(t-2T)} - 1} \quad (5)$$

continued periodically. The parameter $1/a$ sets the length of the crossover intervals. The choice $a=69.1$ ensures that the time needed to decay below vortex strength 10^{-3} is 0.1 dimensionless time unit. Initially vortex 1 is in the midpoint of its inactive interval, vortex 2 is about to die out, vortex 3 is facing time T in its active phase, etc. Figure 1 shows the time dependence of the different vortex strengths. Point vortices in their inactive phase behave as Lagrangian particles.

The phase space of the N -vortex problem is $2N$ dimensional. There exist, in the permanent case, conserved quantities. One of these is the vortex interaction energy

$$\mathcal{E}(t) = - \sum_{j \neq i}^N K_i(t) K_j(t) \ln r_{i,j}(t). \quad (6)$$

This is independent of time if all the K_i are constant [1,8]. In the blinking vortex dynamics the energy \mathcal{E} is, however, time-dependent.

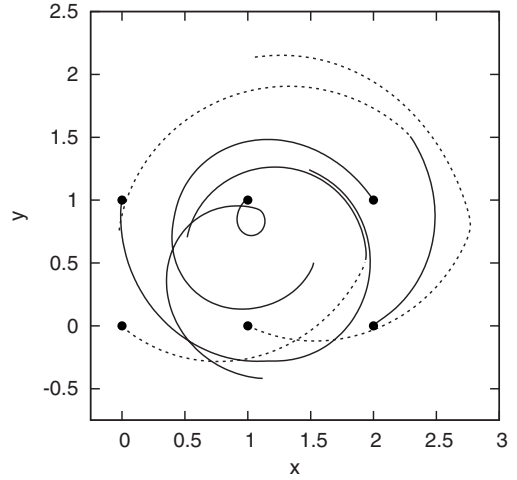


FIG. 2. Vortex trajectories in the time interval ($0 < t < 2$) for $T=1$. The initial conditions are marked by black dots. Solid and dashed lines show the trajectories in the active and inactive periods.

III. NUMERICAL RESULTS

Equations (2)–(5) have been solved by a fourth-order Runge-Kutta algorithm of fixed time step, 10^{-2} . The initial conditions for vortex 1–6 are

$$\vec{x}_0 = ((0,0), (1,0), (2,0), (0,1), (1,1), (2,1)) \quad (7)$$

as illustrated by Fig. 2. These initial conditions were used for both the nonblinking and the blinking six-vortex systems examined in this paper. In the four-vortex case the initial condition was generated by omitting vortices 1 and 2. Furthermore, if not mentioned explicitly, a blinking period of $T=5$ will be assumed. Figure 2 also shows the complex form of the individual vortex trajectories over two blinking times, $2T$, which can have a strong curvature at integer multiples of the blinking time T when vortices are born and die out.

The vortex energy (6) turns out to be a piecewise constant function of time as illustrated by Fig. 3(a). In time intervals when there are exactly four vortices active, \mathcal{E} does not change, but it exhibits a jump whenever a new vortex is born. The energy function consists thus of plateaus of length T . Large jumps upwards correspond to cases when a revived vortex happens to appear close to an already existing one. The small spikes visible in Fig. 3(a) belong to the short crossover intervals of length $1/a$ when five vortices can co-exist. Already on a short time scale a slight average decrease of energy can be observed.

To characterize the overall size of the vortex system, we introduce the diameter

$$d(t) = \max[r_{i,j}(t)], \quad (8)$$

where the pairwise distances $r_{i,j}$ are given by Eq. (3). As another drastical difference with the traditional vortex dynamics, we find that the diameter changes irregularly, and has a tendency to *increase* [see Fig. 3(b)]. This is qualitatively explained by observing that in the nonblinking problem advected particles, and inactive vortices, can depart further away from the vortex center than the vortices themselves (see Fig. 8). Whenever a vortex becomes inac-

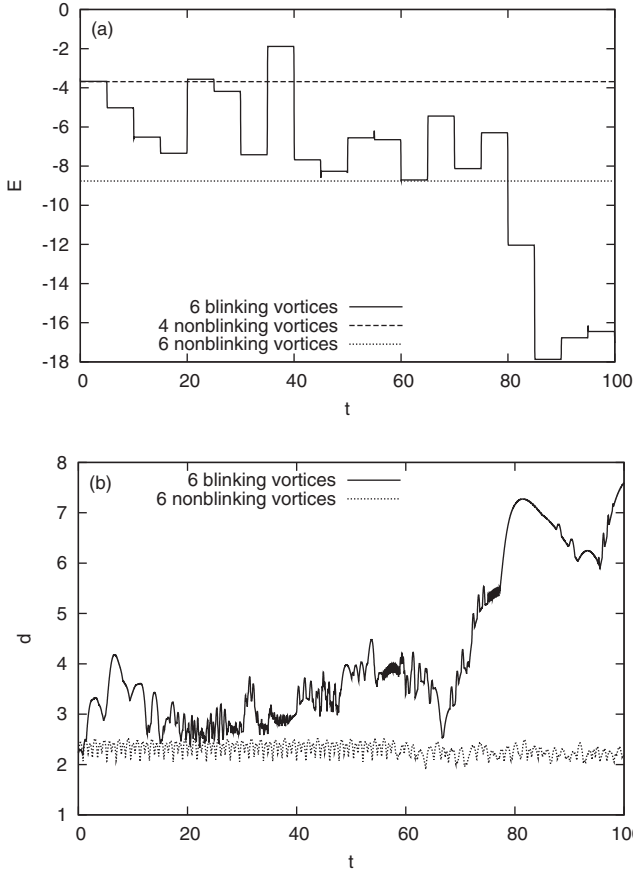


FIG. 3. Energy (a) and diameter (b) of the blinking and nonblinking vortex problem on short time scales ($T=5$).

tive, it can depart and upon its revival, the vortex diameter becomes larger.

A detailed investigation of both the diameter and the energy shows that the actual forms depend very sensitively on the initial condition. Therefore in the following we will compute averages of quantities over ensembles of initial conditions. Let $\vec{x}(t, \vec{x}_0)$ be the trajectory of the nonblinking problem with initial condition \vec{x}_0 . From it we define the following ensemble of initial conditions:

$$M(n, \tau, \vec{x}_0) = \{\vec{x}(j\tau, \vec{x}_0) | j = 1 \dots n\}, \quad (9)$$

where τ is a fixed time interval. For all averaged quantities shown in this paper we used an ensemble of this type generated by a nonblinking six-vortex system with two permanently inactive vortices ($K_1=K_2=0$). This ensemble has the feature of having a certain initial energy. The parameters were chosen as $n=10\,000$, $\tau=10$, and \vec{x}_0 from Eq. (7). We also used two other ensembles: (i). an ensemble of the same type as above but with $K_1=\dots=K_6=1$, and (ii) an ensemble consisting of small perturbations to the initial condition \vec{x}_0 from Eq. (7). We have found the results to be practically independent of n (when big enough), τ , \vec{x}_0 , and the type of the ensemble used, when the average initial size of the ensemble \bar{d}_0 is fixed (see section on scaling properties)

By considering the ensemble described above we find a bunch of graphs for $d(t)$ and $\mathcal{E}(t)$, which strongly deviate

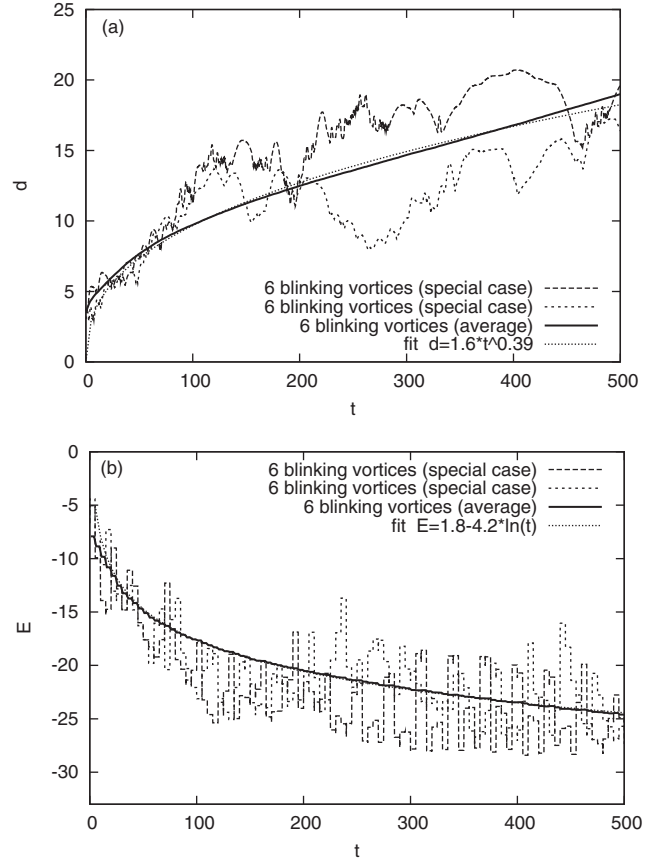


FIG. 4. Diameter (a) and energy (b) of the blinking vortex problem on intermediate time scales ($T=5$). The bold line is the average over an ensemble of initial conditions. The dotted line is a fit which coincides well with the average. The other curves are individual cases and indicate how large the fluctuations around the mean typically are.

from each other. Their arithmetic averages appear, however, to be rather smooth (Fig. 4).

An interesting feature of the diameter's increase is that it follows a power law on time scales $50 < t < 500$ [see Fig. 4(a)]. The average diameter $\bar{d}(t)$ is found to follow the fit $\bar{d}(t) \sim t^\sigma$ valid with $\sigma \approx 0.39 \pm 0.02$, while the average of the squared diameter scales with approximately twice of this exponent $\overline{d^2}(t) \sim t^{\sigma'}$, $\sigma' \approx 0.78$. The spreading of the blinking vortex system is thus an anomalous diffusive process [9] on this time scale. Furthermore, we found for the average energy $\bar{\mathcal{E}}(t) \sim \ln(t)$ [Fig. 4(b)]. In the following we will mainly examine the blinking system only up to intermediate times ($t < 500$). As for the long time behavior, see the Discussion and the Appendix.

The expansion can be interpreted in terms of a simple model. The basic observation is that the overall flow around the vortices at the instant of the n th blinking is approximately K/d_n where d_n is the diameter at this instant. During the next period the diameter changes thus with a velocity proportional to $1/d_n$. Whether there is an increase or a decrease is a random process. Therefore we can write

$$d_{n+1} = d_n + \frac{cT}{d_n} \xi_n, \quad (10)$$

where ξ_n is a random number which takes on values $+1$ and -1 randomly. Since the probability of increase is larger, we assume that these values are taken with probability $p > 1/2$ and $1-p$, respectively. After long times the overall change is small, and d_n can be approximated by a continuous function $d(t)$, $(d_{n+1} - d_n)/T$ by its time derivative \dot{d} . From Eq. (10) we then obtain $\dot{d} = c\xi(t)/d$, from which $\frac{d}{dt}d^2 = 2c\xi(t)$. Since the average of ξ is $p - (1-p) = 2p - 1$ we see that the time derivative of $\overline{d^2}(t)$ is constant which leads to $\overline{d^2}(t) \sim t$, $\overline{d}(t) \sim t^{1/2}$. Deviations from this mean-field like model cause the actual exponent of $\overline{d}(t)$ to be less than $1/2$.

IV. THE DEGREE OF CHAOS

We use the Lyapunov exponent to characterize the degree of chaos in the vortex systems [7]. The largest Lyapunov exponent is defined as

$$\lambda = \lim_{t \rightarrow \infty} \frac{1}{t} \ln \frac{|\vec{x}(t) - \vec{x}'(t)|}{|\vec{x}(0) - \vec{x}'(0)|} = \lim_{t \rightarrow \infty} \lambda(\vec{x}_0, t), \quad (11)$$

where $\vec{x}(t)$ and $\vec{x}'(t)$ are trajectories starting infinitesimally close at $t=0$.

In the nonblinking case $\lambda(\vec{x}_0, t)$ converges to a nonzero positive value, whereas in the blinking case there is a steady decrease of $\lambda(\vec{x}_0, t)$ and a convergence to zero. The steady decrease of $\lambda(\vec{x}_0, t)$ suggests that the degree of chaos in the blinking system decreases with time. This can be explained by the expansion of the system: as the distances between the vortices become larger, their velocity decreases and the motion of the vortices slows down with time, which leads to a lower degree of chaos. It is the ‘‘expanding universe’’ of the blinking vortices which leads to the permanent temporal decay of the largest Lyapunov exponent.

To describe this decrease of chaos we use the concept of finite size Lyapunov exponents [10,11]. Let $\vec{x}(t)$ be the trajectory starting at $t=0$ at \vec{x}_0 and $\vec{x}'(t)$ a trajectory starting at $t=t_i$ (initial time) at a distance $\delta_i \ll 1$ from $\vec{x}(t_i)$ [$|\vec{x}(t_i) - \vec{x}'(t_i)| = \delta_i$]. This pair of trajectories is followed until (at a final time t_f) the distance reaches $|\vec{x}(t_f) - \vec{x}'(t_f)| = \delta_f \gg \delta_i$, so that δ_f is yet $\delta_f \ll 1$. With these quantities we define the finite size Lyapunov exponent at point \vec{x}_0 and at time t_i as [10]

$$\mu(\vec{x}_0, \delta_i, \delta_f, t_i) = \frac{1}{t_f - t_i} \ln \frac{\delta_f}{\delta_i}. \quad (12)$$

For every initial condition \vec{x}_0 we compute a time series $\mu(t_i^n)$ for different t_i 's by the following procedure: after the distance δ_f has been reached, the next initial time and the initial condition of the next $\vec{x}'(t)$ are chosen as

$$t_i^n = t_f^{n-1}, \quad (13)$$

$$\vec{x}'_n(t_i^n) = \vec{x}(t_i^n) + \frac{\delta_i}{\delta_f} [\vec{x}(t_i^n) - \vec{x}'_{n-1}(t_i^n)]. \quad (14)$$

This choice of $\vec{x}'_n(t_i^n)$ ensures that $|\vec{x}(t_i^n) - \vec{x}'_n(t_i^n)| = \delta_i$ and that the direction of $\vec{x}(t_i^n) - \vec{x}'_n(t_i^n)$ is parallel to that of $\vec{x}(t_f^{n-1})$

$-\vec{x}'_{n-1}(t_f^{n-1})$. With these rules the following relation holds between λ and μ :

$$\lambda(\vec{x}_0, t) = \sum_{n=0}^N \frac{t_f^n - t_i^n}{t} \mu(\vec{x}_0, t_i^n), \quad (15)$$

where $t_i^0 = 0$ and $t_f^N = t$. This relation is true for every choice of $\delta_i, \delta_f \ll 1$ and shows that λ is a weighted time average of μ .

The time series $\mu(\vec{x}_0, t_i^n)$ characterizes the degree of chaos at time instants t_i^n ($0 \leq n \leq N$). The quantities $\lambda(\vec{x}_0, t)$ and $\mu(\vec{x}_0, t_i^n)$ converge to zero for $t \rightarrow \infty$. For the average $\overline{\mu}(t) = \langle \mu(\vec{x}_0, t_i^n = t) \rangle_{\vec{x}_0}$ we have found a power law to be valid ($50 < t < 500$),

$$\overline{\mu}(t) \sim t^{-0.39}. \quad (16)$$

To compare the blinking and nonblinking systems we examine the energy dependence of μ . In the nonblinking case the energy \mathcal{E} depends only on the initial condition \vec{x}_0 but not on the time. Therefore to get $\mu(\mathcal{E})$ we generate an initial condition \vec{x}_0 with a certain energy \mathcal{E} and assign

$$\mu(\mathcal{E}, t_i^n) = \mu(\mathcal{E}(\vec{x}_0, t_i^n)) = \mu(\vec{x}_0, t_i^n). \quad (17)$$

This quantity still has a time dependence. For a certain energy $\mu(\mathcal{E}, t)$ oscillates around some mean value. Therefore we compute a time average:

$$\overline{\mu}(\mathcal{E}) = \lim_{t \rightarrow \infty} \sum_{n=0}^{N(t)} \frac{t_f^n - t_i^n}{t} \mu(\mathcal{E}, t_i^n). \quad (18)$$

Within an ergodic component of the phase space of the nonblinking problem this can also be considered as an ensemble average. It follows from Eq. (15) that $\overline{\mu}(\mathcal{E})$, in the nonblinking case, is indeed the energy-dependent Lyapunov exponent $\lambda(\mathcal{E})$.

In the blinking case \mathcal{E} depends both on time and initial condition. To get $\mu(\mathcal{E})$ in this case we consider the time dependence of \mathcal{E} :

$$\mu(\vec{x}_0, \mathcal{E}) = \mu(\vec{x}_0, \mathcal{E}(t_i^n)) = \mu(\vec{x}_0, t_i^n). \quad (19)$$

Furthermore, we compute an ensemble average over the initial conditions:

$$\overline{\mu}(\mathcal{E}) = \langle \mu(\vec{x}_0, \mathcal{E}) \rangle_{\vec{x}_0}. \quad (20)$$

This kind of averaging is also used by meteorologists in their ensemble forecasting method [12].

Figure 5 shows $\overline{\mu}(\mathcal{E})$ for the nonblinking four- and six-vortex system and the blinking six-vortex system. In all three cases the degree of chaos decreases as the energy decreases. This is due to the slower motion of the vortices with lower energies. Note that $\overline{\mu}$ has an exponential dependence on \mathcal{E} (Fig. 5). Furthermore, the following inequality holds:

$$\overline{\mu}_4^{\text{nonblinking}}(\mathcal{E}) < \overline{\mu}_6^{\text{blinking}}(\mathcal{E}) < \overline{\mu}_6^{\text{nonblinking}}(\mathcal{E}). \quad (21)$$

From this we conclude that for a given energy \mathcal{E} the blinking six-vortex system is more chaotic than the nonblinking four-vortex system and less chaotic than the nonblinking six-vortex system. This is understandable as in the blinking six-vortex system only four of the six vortices are active at any

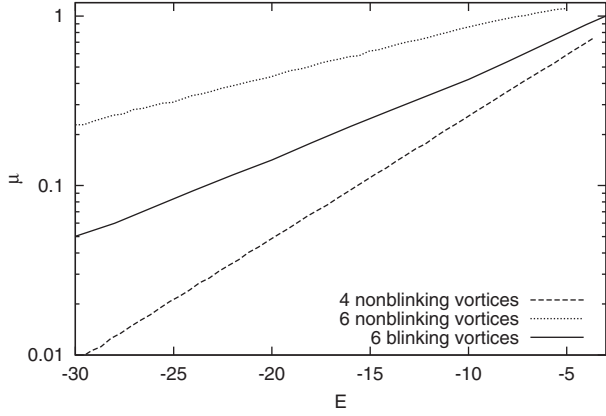


FIG. 5. Energy dependence of the finite size Lyapunov exponent $\bar{\mu}$.

time. The higher degree of chaos compared to a nonblinking four-vortex system is caused by the blinking. The decreasing degree of chaos in a blinking system is due to the expansion.

V. ADVECTION DYNAMICS

Knowing the orbits $(x_i(t), y_i(t))$ of the vortex centers, the velocity field generated by the vortices is obtained via Eq. (1) in an arbitrary point (x, y) (outside of the vortex centers) as [1,8]

$$v_x(x, y, t) = - \sum_{i=1}^N K_i(t) \frac{y - y_i(t)}{r_i^2(t)}, \quad v_y(x, y, t) = \sum_{i=1}^N K_i(t) \frac{x - x_i(t)}{r_i^2(t)}, \quad (22)$$

where $r_i(t) = \sqrt{[x - x_i(t)]^2 + [y - y_i(t)]^2}$ is the distance of point (x, y) from vortex i . The time dependence of the full velocity field is therefore of similar character as the dynamics of the vortex centers.

The equation of an advected particle in the velocity field of N vortices expresses the fact that the velocity of an advected particle is the same as that of the flow at the same location. Thus in our case with $N=6$

$$\dot{x} = - \sum_{i=1}^6 K_i(t) \frac{y - y_i(t)}{r_i^2(t)}, \quad \dot{y} = \sum_{i=1}^6 K_i(t) \frac{x - x_i(t)}{r_i^2(t)}. \quad (23)$$

This is a two-dimensional motion driven by the dynamics of the vortex centers. Equations (23) have been solved by a fourth-order Runge-Kutta algorithm with time steps of 10^{-2} or 10^{-4} dimensionless time units. The smaller time step was used when the distance between the advected particle and any vortex became smaller than 0.4 length units.

Instead of the advection of a single particle, it is more natural to consider an ensemble of particles since it is this setting which is relevant in the problem of spreading of pollutants [8]. Initially, we consider a localized droplet containing a large number N_0 of particles uniformly distributed, and follow how this droplet becomes deformed and stretched as time goes on. This problem requires the numerical solution of the same set of differential equations with $N_0 \gg 1$ different initial conditions.

Figure 6 shows the time evolution of a droplet of $N_0 = 40\,000$ particles (whose initial shape is given in the inset) as time goes on. The tiny initial droplet is stretched and folded rapidly. The change of the box scale in Fig. 6 clearly indicates the permanent growth of the droplet diameter. Note that the spreading of the droplet is rather inhomogeneous, the pattern is strongly filamentary.

In analogy with diameter d of the vortex system [cf. Eq. (8)], we define the droplet diameter d_d as the maximum distance between two advected particles of the droplet. In particular cases we have found the droplet diameter d_d to be of the same order as the diameter of the vortex system. Therefore we conclude that this is also true for the averaged quantities $\bar{d}_d(t)$ and $\bar{d}(t)$: It is the expansion of the vortex centers that determines the spreading of the droplet that also follows a subdiffusive law.

The dye pattern can be characterized by means of a non-trivial fractal dimension. We evaluated the information dimension D_1 [7,9] based on the number $N_i(\epsilon)$ of dye points falling into box i of linear size ϵ . The value of the dimension then follows from

$$\sum_i \frac{N_i(\epsilon)}{N} \ln \frac{N_i(\epsilon)}{N} \sim D_1 \ln \epsilon \quad (24)$$

for a sufficiently small resolution ϵ . After a few blinks, a nice scaling has been found leading to clearly identifiable D_1 values as a function of time. As Table I indicates, the information dimension increases first, reaches an approximate plateau of height definitely below 2 (in the time interval over which the subdiffusive expansion is valid) and then it falls back. The latter is due to the very long time dynamics that shall be explored in the Discussion and the Appendix.

VI. SCALING PROPERTIES

The exact shape of the expansion curves depends, however, on the blinking period T (see Fig. 7). In the log-log plot of \bar{d} vs the scaled dimensionless time t/T a linear behavior can be seen between $10T$ and $100T$ (for $5 \leq T \leq 15$). The averaged diameter can be written in this range as

$$\bar{d}(t, T) \sim t^{\sigma(T)}, \quad (25)$$

where $\sigma(T)$ is a slowly increasing function of T , with values $0.39 < \sigma < 0.45$.

For times after $100T$ a new phenomenon becomes typical, the separation of a couple of blinking vortices. This can lead to a practically uniform motion of the couple along a straight line, as discussed in the Appendix. The mixture of the subdiffusive expansion and the couple separation leads to a much faster growth of the diameter than $t^{\sigma(T)}$, as can be seen in Fig. 7 for $t > 100T$.

We have found that the shape of the expansion curves depends in a nontrivial way on the average initial size of the ensemble $\bar{d}_0 = \bar{d}(0)$. It turns out that the combined parameter T/\bar{d}_0^2 determines the shape of the expansion curve. This can be seen by noting the invariance of Eq. (2) under the transformation $\bar{x} \rightarrow \alpha \bar{x}$, $t \rightarrow \alpha^2 t$, for $\alpha > 0$. This suggests the exist-

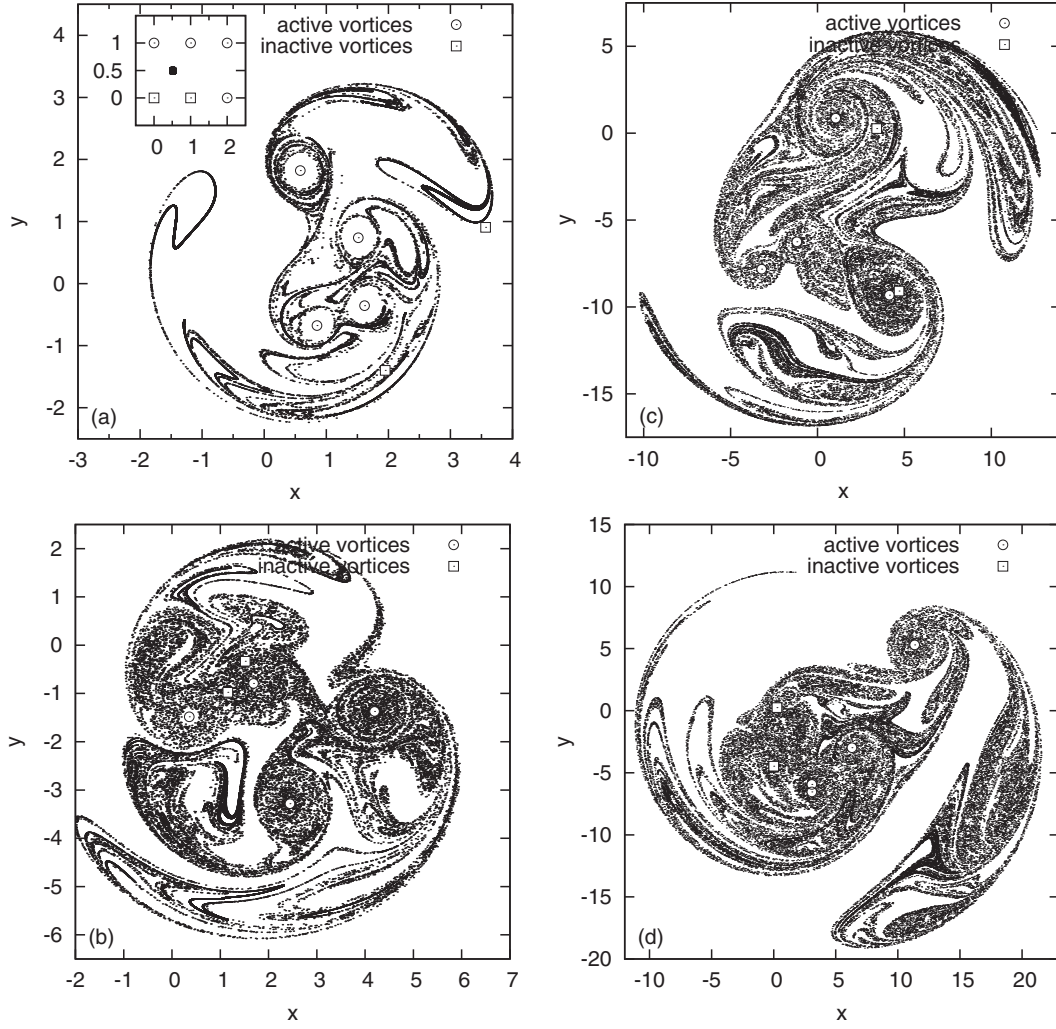


FIG. 6. Shape of a droplet of 40 000 particles for $T=5$ at time $t=9$ (a), $t=49$ (b), $t=249$ (c), and $t=498$ (d). The initial condition of the vortices and the initial shape of the droplet [centered at $(0.5, 0.5)$] are shown in the inset of (a).

tence of a scaling law with a universal function D ,

$$\bar{d}(\bar{d}_0, T, t) = \bar{d}_0 D\left(\frac{T}{\bar{d}_0}, \frac{t}{\bar{d}_0^2}\right). \quad (26)$$

Numerically, this form has been found to be valid with a very high accuracy. In the scaling regime then

$$\bar{d}(\bar{d}_0, T, t) \sim t^{\sigma(\bar{d}_0, T)} \quad (27)$$

and

$$\sigma(\bar{d}_0, T) = \sigma(T/\bar{d}_0^2). \quad (28)$$

We note that the parameter T/\bar{d}_0^2 can be understood as the ratio of two time scales: the blinking time scale T and the

“dynamical time scale” $\bar{d}_0^2 \sim \bar{d}_0/(K/\bar{d}_0) = \bar{d}_0/v(\bar{d}_0)$ with $v(\bar{d}_0)$ being the typical velocity at a distance \bar{d}_0 . The longest time interval with power law scaling is found for $T/\bar{d}_0^2 \approx 1$

To check the robustness of the results we studied the influence of parameters. We have found that the value of parameter a [see Eq. (5)], which sets the crossover time scale $1/a$, has no effect on the expansion curves (Fig. 7), as long as $1/a$ is very small compared to T [i.e., $1/(aT) < 0.01$]. For $1/a$ not very small, the exact shape of the expansion curves changes, but qualitative aspects stay the same, in particular, $\sigma(T/\bar{d}_0^2)$ does not change with a . Moreover, this exponent remains unchanged even if the crossover function $K(t)$ in Eq. (5) takes other forms. Preliminary investigations also show that the number N of blinking vortices does not play a role,

TABLE I. Time dependence of the information dimension D_1 of the droplet shown in Fig. 6.

t	10	20	50	100	200	500	1000	2000	4000
D_1	1.25	1.49	1.60	1.71	1.70	1.75	1.76	1.71	1.66

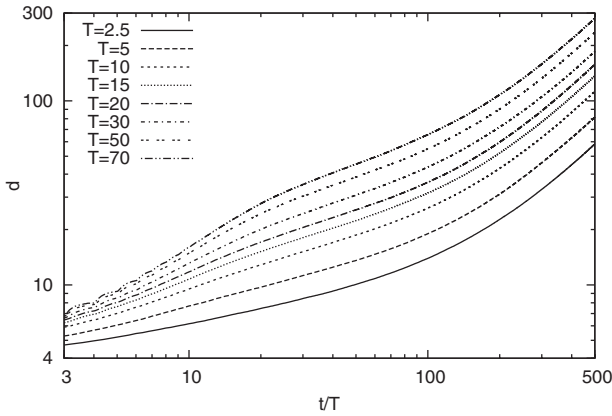


FIG. 7. Time dependence of the averaged diameter $\bar{d}(t)$ of the blinking vortex problem for different blinking times T , represented as a function of t/T in a log-log plot. The initial size of the ensemble used for averaging is $\bar{d}_0=3.66$.

$\sigma(T/d_0^2)$ remains unchanged when N takes values up to $N=12$.

VII. DISCUSSION

We have shown that the dynamics of blinking vortices is more complex than that of classical point vortices. The average size of the blinking system increases with time, in a subdiffusive way.

Advection takes place in the “expanding universe” of the blinking vortices. Therefore the average size of the advection pattern also increases in time, in the same fashion as the size of the vortices. This feature should be contrasted with advection patterns generated by classical point vortices. It is clear from Fig. 8 that outside a circle of radius of order unity, the advection dynamics is nonchaotic, mixing is rather poor. Furthermore, around the fixed vortices “vortex cores” are formed which are not accessible by particles initiated out-

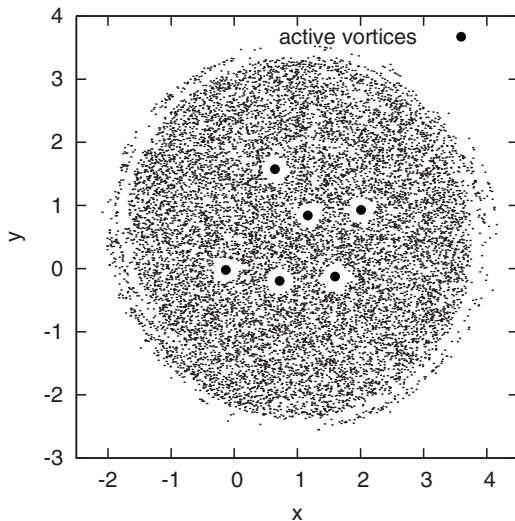


FIG. 8. Shape of the same droplet as in Fig. 6 for six nonblinking vortices at time $t=498$.



FIG. 9. (Color online) Pollen seeds on a fluid surface (on a side branch of River Danube, Hungary). From [18], with permission of M. Pattantyús-Ábrahám.

side. These cores are characterized by very fast fluid rotation [13,14], and their external boundary is, in the language of dynamical systems, a Kolmogorov-Arnold-Moser (KAM) surface [7,8]. Such cores are not present at all in the blinking problem, since cores of active vortices are converted into normal fluid regions, whenever the vortex becomes inactive. Around the vortices, mixing is more homogeneous than in the classical problem. On the other hand, mixing is not pronounced in certain regions due to the permanent expansion of the system, and the pattern is therefore more filamentary. Such filamentary advection patterns of dimension strictly lower than 2 have only been observed in open flows, where there is a material current flowing through the region of observation [15]. In the context of traditional vortices open flow situation arises if the overall vortex strength is zero [16,17]. The expanding universe of the blinking vortices is thus in between the cases of closed and open flows since an approximate rescaling of the size [a shrinking proportional to $1/d(t)$] would lead to a material current inward the system. The dye pattern of the blinking vortex problem is more complex than that of the traditional problem. It does not contain cores, is highly filamentary, and is therefore similar to patterns, see, e.g., Fig. 9, observable in nature.

Finally we note that certain features of the scaling behavior are similar to what has been found in *decaying* two-dimensional turbulence [19–21]. In such cases, vorticity is distributed in the full fluid domain of observation, but due to the lack of any external driving, vortices merge and their mean distance increases as time goes on. There the average number of vortices decays in time according to a power law with an exponent in the range 0.67–0.77 [19–21], while the mean separation between vortices increases with an exponent 0.38 [19]. In our setting the latter corresponds to the scaling of \bar{d} , while the former to that of N/\bar{d}^2 . The exponents would thus be σ and 2σ , respectively. Typical values of σ are close to those measured in turbulence, but the fact that the exponent also depends on the initial size is specific to our model, which cannot be present in studies of extended (but decaying) turbulence.

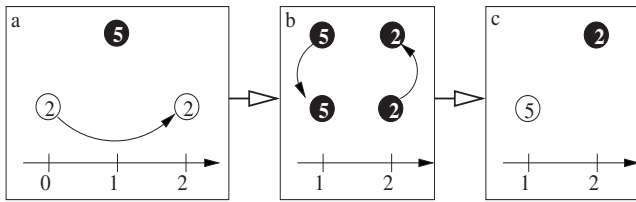


FIG. 10. Motion of the vortex couple formed by vortex 2 and 5 in the absence of any other vortices. Length unit along the axis is $r_0/\sqrt{2}$. Black (white) circles denote active (inactive) vortices, and the cross represents the vortex center.

This suggests that the dynamics of blinking vortices may be a model of how a strong localized perturbation spreads in an ambient fluid at rest, i.e., how turbulent spots evolve in two-dimensional flows, on a time scale where dissipative effects are negligible.

ACKNOWLEDGMENTS

The authors are indebted to the Max Planck Institute for the Physics of Complex systems, Dresden, for the hospitality. We thank Margit Pattantyús-Ábrahám for permitting us the use of her photo, and József Vanyó for valuable remarks. One of us (T.T.) acknowledges useful discussions with A. Provenzale. This research has been supported by OTKA Grant No. T047233.

APPENDIX: DYNAMICS OF BLINKING VORTEX COUPLES

In a traditional nonblinking vortex system a uniform motion of a vortex couple can only be observed, when the total vorticity of the couple is zero [1]. In a blinking system, however, we have found uniform motion of vortex couples with nonzero total vorticity. This effect plays a dominant role in the long time expansion of the blinking vortex system.

In the following a short explanation of the motion of an isolated vortex couple will be given. Let us consider vortex number 2 and 5 (or 1 and 4, or 3 and 6) from our blinking six-vortex system (see Fig. 1 with $a=\infty$). At $t=0$ vortex 2 is inactive and rotates around vortex 5 with the rotation period $\tau=2\pi r^2$, where r is the distance between the vortices. Let us choose r so that $\tau=8T$ (T =blinking period), which we will call the resonant distance $r_0=\sqrt{4T/\pi}$. With this choice vortex 2 makes a quarter rotation around vortex 5 during his inactive phase of length $2T$ [Fig. 10(a)]. When it is activated,

both vortices rotate around their vortex center for time T with the rotation period $\tau'=\tau/2=4T$ [Fig. 10(b)]. Then vortex 5 is deactivated [Fig. 10(c)] and the configuration of the vortices is the same as at the beginning (besides that the vortices are interchanged), hence the same procedure starts again. During such a period the vortex couple passes a distance $r_0/\sqrt{2}$ in the x direction. Therefore the velocity of the vortex couple is constant, $v_0=[2/(9\pi T)]^{1/2}$. The straight motion in one direction only happens at the resonant distance r_0 of the vortices. A larger or smaller distance leads to a curvature of the path to the right or the left, respectively. The curvature of the path increases with an increasing deviation from r_0 . We have found that the resonant distance r_0 is the same for all possible vortex couples (e.g., 1 and 2) although the mechanism is slightly different.

Until now we have neglected the influence of other vortices on such a vortex couple. Let us consider the other four vortices of our blinking six-vortex system to be far away from the vortex pair. Then the displacement of the vortex couple due to the flow generated by the other four vortices (direct influence) is very small and negligible. But there is also an indirect influence: The flow of the other vortices causes a very small variation of the distance r between the vortices. The couple reacts very sensitively on such variations of r . The effect depends both in sign and magnitude on the orientation of the couple's motion relative to the other four vortices. This and the fact that the difference $r-r_0$ determines the curvature of the path, and therefore the future direction of movement, leads to a feedback. Hence many different types of paths are possible: wavy motion in one direction, closed circles of large radius, etc.

We have found that this indirect interaction between a vortex couple and the rest is by far more long ranged than the direct and obvious interaction. It affects the motion of the couple at distances, where one would not expect any effect of velocity field, that goes as $1/r$.

The effect of a moving vortex pair dominates the long time expansion of the blinking six-vortex system. At a certain time, which depends on the initial condition, but is on average around $100T$, a vortex couple separates and moves away from the rest with constant velocity. This leads to a roughly linear expansion of the system. The separation and motion of couples is an interesting and also unexpected effect of the blinking model. But as we do not see this feature to characterize any real vortex systems, we restricted our study of the blinking vortices up to times, where no vortex couple separation occurs.

[1] P. Newton, *The N-Vortex Problem* (Springer, Berlin 2001).
 [2] H. Aref, *J. Fluid Mech.* **143**, 1 (1984).
 [3] H. Aref, S. W. Jones, and I. Zawadski, *Physica D* **37**, 423 (1989).
 [4] G. Károlyi and T. Tél, *Phys. Rep.* **290**, 125 (1997).
 [5] D. Elhmaildi, A. Provenzale, and A. Babiano, *J. Fluid Mech.* **257**, 533 (1993).

[6] A. Babiano, G. Boffetta, A. Provenzale, and A. Vulpiani, *Phys. Fluids* **6**, 2465 (1994).
 [7] E. Ott, *Chaos in Dynamical Systems* (Cambridge University Press, Cambridge, England, 1993).
 [8] T. Tél and M. Gruijz, *Chaotic Dynamics* (Cambridge University Press, Cambridge, England, 2006).
 [9] T. Vicsek, *Fractal Growth Phenomena* (World Scientific, Sin-

- gapore, 1989).
- [10] E. Aurell, G. Boffetta, A. Crisanti, G. Paladin, and A. Vulpiani, *J. Phys. A* **30**, 1 (1997).
- [11] G. Boffetta, G. Lacorata, G. Redaelli, and A. Vulpiani, *Physica D* **159**, 58 (2001).
- [12] M. Pena and E. Kalnay, *Nonlinear Processes Geophys.* **11**, 319 (2004).
- [13] L. Kuznetsov and G. M. Zaslavsky, *Phys. Rev. E* **58**, 7330 (1998).
- [14] L. Kuznetsov and G. M. Zaslavsky, *Phys. Rev. E* **61**, 3777 (2000).
- [15] T. Tél, A. P. S. de Moura, C. Grebogi, and G. Károlyi, *Phys. Rep.* **413**, 91 (2005).
- [16] Á. Péntek, T. Tél, and Z. Toroczkai, *J. Phys. A* **28**, 2191 (1995).
- [17] Z. Neufeld and T. Tél, *Phys. Rev. E* **57**, 2832 (1998).
- [18] M. Pattantyús-Ábrahám, Ph.D. thesis, Budapest University of Technology and Economics (in Hungarian), 2008.
- [19] A. E. Hansen, D. Marteau, and P. Tabeling, *Phys. Rev. E* **58**, 7261 (1998).
- [20] A. Braco, J. C. McWilliams, G. Murante, A. Provenzale, and J. B. Weiss, *Phys. Fluids* **12**, 2931 (2000).
- [21] J. P. Laval, P. H. Chavanis, B. Dubrulle, and C. Sire, *Phys. Rev. E* **63**, 065301(R) (2001).